Research Square

Preprints are preliminary reports that have not undergone peer review.
They should not be considered conclusive, used to inform clinical practice,
or referenced by the media as validated information.

Experimental study on injection of ferrous sulphate for remediation of a clayey soil contaminated with hexavalent chromium

Guang Hu
Central South University
Yong He (heyong18@csu.edu.cn)
Central South University https://orcid.org/0000-0001-9653-6624
Kao-fei Zhu
Central South University
Zhao Zhang
Central South University
Wei Lou
Central South University
Ke-neng Zhang
Central South University
Yong-gui Chen
Tongji University
Qiong Wang
Tongji University

Research Article

Keywords: Hexavalent chromium, Soil remediation, Ferrous sulphate, Clayey soil, Pressure injection

Posted Date: June 3rd, 2022

DOI: https://doi.org/10.21203/rs.3.rs-1637559/v1

License: This work is licensed under a Creative Commons Attribution 4.0 International License.
Read Full License

Version of Record: A version of this preprint was published at Environmental Earth Sciences on March 29th, 2023. See the published version at https://doi.org/10.1007/s12665-023-10853-y.

Abstract

In-situ remediation of the Cr( ) contaminated clayey soil remains challenging due to the low hydraulic conductivity and high ion adsorption capacity of the clays. In this study, the injection tests of ferrous sulphate ($FeSO_4$) for a clayey soil contaminated with hexavalent chromium (Cr( )) were performed to explore the feasibility of $FeSO_4$ solution for remediation of Cr( ) contaminated soil under different injection pressures. The results show that the injection of $FeSO_4$ solution under the pressure of 30 kPa, 70 kPa, and 100 kPa caused the hydraulic conductivities of the specimens to decrease by 36.5%, 38.7% and 32.2%, respectively. This phenomenon could be attributed to the formation of the mixed iron( )/chromium( ) hydroxide, a process for which scanning electron microscopy with energy-dispersive X-ray microanalysis provided direct evidence. Moreover, the mobility capacity of Fe( ) was stronger under high pressure (70 kPa, 100 kPa) as indicated by Fe profiles in specimens after remediation under different injection pressures. The range of iron increment at 100 kPa was 3.2–11.9 (g/kg). However, the maximum iron increment at 30 kPa was only 5 (g/kg) and the migration of Fe( ) was limited, which was less than 2.5 cm. In addition, the injection pressure of 70 kPa was the most efficient for remediation of Cr( ) contaminated soil under the experimental condition in present work, which the remediation efficiency was 87.43%-95.12%. As injection pressure increased, Cr( ) leaching increased. Therefore, these experimental results can be used as a reference for remediation of chromium contaminated soil by in-situ injection.

1 Introduction

With the rapid development of global industrialization and urbanization, the pollution of heavy metal in soil and groundwater has become increasingly serious [1]. According to incomplete statistics, more than 5 million sites are contaminated with heavy metals around the world, resulting in over 20 million hectares to be remedied [2]. At present, there are as many as 450,000 and 342,000 contaminated sites in North America and Europe, while the number of remaining contaminated sites in China has exceed more than 500,000 owing to the upgradation of industrial structure and the transformation of economic growth [3, 4]. Global mining activities, steel and chemical industrial production, and excessive use of chemicals have caused the continuous accumulation of Chromium (Cr) in the environment, seriously threatening environmental quality and public health [5, 6].

Generally, chromium in soil mainly exists in the trivalent form, Cr( ), and the hexavalent forms, as chromate (CrO_4^{2-}) or dichromate ($Cr_2O_7^{2-}$) [7]. Different species of chromium have different mobility and toxicity. Cr( ) generally comes from rock weathering, and it is easy to form precipitation under circumneutral pH, which means that it is the most thermodynamically stable species and difficult to migrate in reducing conditions [8]. Cr( ) is low toxicity and it's an essential trace element for human beings or a nutrient for plant growth [9, 10]. In contrast to Cr( ), Cr( ), a highly water-soluble and fluid substance, is a dangerous chemical substance with mutagenic and carcinogenic properties, resulting in 100–500 times toxicity of Cr( ) [11, 12]. Cr( ) are non-biodegradable, and hence, can accumulate continuously in the environment and the living organisms, which can easily cause adverse effects on the

organs and tissues of human body. It is also the second most abundant inorganic contaminant at contaminated sites as reported by the National Academy of Sciences Committee on Groundwater Cleanup [13]. Therefore, developing efficient techniques for remediation of Cr( ) contaminated soil is an important task for protecting public health and the environment.

Numerous methods have been proposed to reduce the concentration or solidify/stabilize the contaminant in the environment, including physical (e.g., soil turning over, soil changing, topsoil removal, heat treatment, electrokinetic), chemical (e.g., leaching, redox reaction), and biological (e.g., microbial remediation) remediation methods [14–16]. In recently years, in-situ injection technologies that make use of nano zero valent iron [17] or bivalent iron [18] as ferrous sulphate materials for the remediation of Cr( ) contaminated soils have rapidly developed. Several studies performed during the past have already demonstrated the feasibility of ferrous sulphate for remediation of aquifer, coarse soil contaminated with Cr( ) and chromite ore processing solid waste by a lab-scale test or a field trial [19–22]. In general, most of the literatures concentrate on using ferrous sulphate for remediation of coarse soils contaminated with Cr( ) or only on a batch scale in the aqueous phase. Few literatures discuss the remediation of clayey soil contaminated with Cr( ) by injection of ferrous sulphate under different pressures. Thus, the objective of this work is to evaluate the effect of injection pressures on remediation of low permeability clayey soil contaminated with Cr( ).

In this study, a silty clay was collected from a ferrochrome alloy plant in Xiang-xiang, Hunan Province, China (Fig. 1), and laboratory tests using a self-designed injection system were conducted to evaluate the remediation effects of ferrous sulphate for a Cr( ) contaminated clayey soil. The change of hydraulic conductivity of Cr( ) contaminated soil under the injection of ferrous sulphate solution and distilled water was studied. Moreover, the concentrations of Cr( ) and total Cr in soil at different depths were determined, and the the effects of different injection pressures on the migration and distribution of Fe at soils were revealed. In addition, remediation efficiencies of Cr( ) in soil at different depths were calculated based on the experimental results under different injection pressures. Scanning electron microscopy with energy-dispersive X-ray spectroscopy (SEM-EDX) was also carried out to obtain the surface morphology characteristic of the soil. The results of this study can help us to better understand the mobility and interaction of the reducing agent with the contaminant and contribute to implementing the in-situ injection technology on a real scale for remediation of contaminated sites.

2 Materials And Methods

2.1 Materials

The soil was an uncontaminated silty clay soil, collected nearby a ferrochrome alloy plant, a Cr( ) contaminated site, in Xiang-xiang, Hunan Province, China, at depth between 0.50 and 2.00 m. The location is shown in Fig. 1. Some physical-chemical and geotechnical characteristics of this soil were tested per GB/T 50123 – 2019, and the results are presented in Table S1. As can be seen, the soil is acidic with low permeability. The chemical components of it were analyzed by X-ray fluorescence spectrometry

(Netherlands, AXIOS mAX) as follows: SiO_2 63.056%, Al_2O_3 19.483%, Fe_2O_3 11.048%, K_2O 1.979%, TiO_2 1.234%, SO_3 1.178%, MgO 0.873%, CaO 0.222%, Na_2O 0.200%, P_2O_5 0.119%, MnO 0.083%, ZnO 0.064%, others 0.461. The ferrochrome alloy plant was built in 1958, put into operation in 1962, and shut down in 2010. From top to bottom, the major lithologies in the Cr( ) contaminated site are miscellaneous fill, silty clay, medium silty gravel, and mudstone. There was a chromium hydrometallurgical smelting production line in the ferrochrome alloy plant. The long-term production and the random stacking of chromium slag resulted in serious Cr(VI) pollution of the silty clay layer and groundwater in the study area.

The ferrous sulphate solution, which was prepared by dissolving some iron sulphate heptahydrate in distilled water, was used in the injection tests for remediation of Cr( ) contaminated soil. Iron sulphate heptahydrate used in this study was analytical grade and 99% purity and bought from the Sinopharm Chemical Reagent Co., Ltd. (Shanghai, China). Palma et al. [22] demonstrated that the removal efficiency of Cr( ) achieved the highest when the molar ratio of Fe( ) in solution to Cr( ) in soil specimen was 30:1. Considering that the reduction of Cr( ) by injecting $FeSO_4$ solution into a compacted clayey soil was different from the batch model by adding $FeSO_4$ to a certain amount of bulk soil specimen, the concentration of $FeSO_4$ adopted in this study was doubled to 50 g/L.

2.2 Test equipment

The injection system was self-designed and developed (as shown in Fig. 2). The main components include a confining pressure system, an injection pressure controller, a pressure chamber and a chemical solution converter. The chemical solution converter converts the water pressure provided by the pressure /volume controller into the pressure of the chemical solution. The system is equipped with three independent systems for controlling axial pressure, confining pressure and injection pressure. The axial deformations of soil specimens were determined by a dial gauge.

Two pressure/volume controller apparatus were used as confining pressure control system and injection pressure control system, respectively (as shown in Fig. 2). The pressure/volume controller is a screw pump controlled by a microprocessor, which can apply 0–2.0 MPa independent injection pressure or confining pressure to the soil specimens. It can also display the volume and pressure value during the test period to monitoring the volume change of the soil specimen during the injection process.

The schematic diagram of the chemical solution converter is shown in Fig. 2. There is a diaphragm inside the chamber. The upper part of the diaphragm was filled with the injection solution, and the lower part was filled with distilled water. The injection pressure control system applied pressure to the distilled water in the chamber of the lower part of the diaphragm, and the pressure was transmitted to the injection solution through the diaphragm. A pipe was used to connect the injection solution outlet of the chemical solution converter with the injection solution inlet at the bottom of the triaxial pressure chamber, and the pressurized injection solution was transferred from the bottom of the specimen to the top of that through the porous stone at the bottom of the triaxial chamber.

2.3 Specimen preparation

The Cr( ) contaminated soils used in injection tests were artificially prepared. Firstly, the uncontaminated soil was dried, grounded and sieved using a 0.5 mm aperture sieve. After that, uncontaminated soil (1000 g) was placed in a polyethylene container and the predetermined mass of potassium dichromate solution ($K_2Cr_2O_7$) was added and homogenized to bring the concentration of Cr ( ) to 1000 mg·kg^{-1}. 2.829 g of $K_2Cr_2O_7$ was dissolved in 80 ml distilled water. The prepared solutions were then sprayed and mixed thoroughly with soil layer by layer in the polyethylene container. Next, the contaminated soil specimens were cured in a sealed bag at room temperature (20°C) for 7 days. The moisture content of contaminated soil specimens was determined, which was 8.27%. Through concentration analysis, the actual concentrations of Cr( ) and Cr(Total) in the contaminated soil used in this study were 832 mg/kg and 1100 mg/kg, respectively.

The specimen preparation procedure is shown in Fig. S1. The contaminated soil specimens (Fig. S1a) with an initial moisture content of 8.27% were compacted to specimens with a height and diameter of 50 mm and dry density of 1.5 g/cm^3 (Fig. S1c) by using the static compaction method (Fig. S1b). Details of this method are available in [23, 24].

2.4 Injection test

In present work, the relative content of exchangeable fraction chromium was high because the contaminated soil specimens were artificially prepared. If only $FeSO_4$ solution is injected, it is not clear whether the decrease in Cr( ) was caused by reduction to Cr( ) or by leaching. Thus, the distilled water was also used in the injection test as a control. The as-compacted specimen (Fig. S1c) was installed in the pressure chamber as shown in Fig. 2. Filter papers and porous stones were placed on the top and bottom of the specimen, respectively. The pressure chamber was filled with water and the internal air was evacuated. The chamber at the upper part of the diaphragm of chemical solution converter was filled with $FeSO_4$ solution, and the lower chamber was filled with distilled water. After that, the injection system was assembled as shown in Fig. 2. The axial pressure and confining pressure of the specimen were applied and maintained to 200 kPa and 130 kPa, respectively, considering the K_0 stress state of the specimen. Then, the vertical deformation of the specimen after applying axial pressure and confining pressure was monitored by a dial gauge. When the vertical deformation was stable, different injection pressures (30 kPa, 70 kPa, 100 kPa) were applied to generate an injection flow, resulting in $FeSO_4$ infiltration from the bottom to the top of the specimen. For each group of injection pressure, a control test was conducted by injecting distilled water with remaining the rest of the conditions unchanged. According to Darcy's law, the expression for the hydraulic conductivity is

$$k = \frac{q}{Ai} = \frac{\Delta V L}{A t \Delta h} \quad (1)$$

where k is hydraulic conductivity (cm/s), q is injection flow (cm^3/s), i is hydraulic gradient, A is cross sectional area of specimens (cm^2), L is the specimen height (cm), V is the volume of solution flowing through the specimen in time t (cm^3), Δ h is head difference (cm), t is time (s).

In order to evaluate the remediation effect of $FeSO_4$ under different injection pressures, the injection tests were ended after 24 hours. The specimen was taken out of the pressure chamber and sliced into 4 equal parts along the injection flow direction, each equal to 1.25 cm. The average metal concentration (Cr( ), Cr(Total), Fe(Total)) in each part corresponds to the metal concentration at different depths of the specimen (1.25, 2.5, 3.75, 5.0 cm, in relation to the bottom of the specimen).

The concentrations of Cr( ) and Cr(Total) in specimens were determined by atomic absorption spectrophotometry, after alkaline digestion and acid digestion, respectively, according to the method EPA 3060 A and EPA Method 3050 B [25, 26]. The concentrations of Fe at different depths of specimens after acid digestion were determined by inductively coupled plasma optical emission spectrometry (ICP-OES). Based on the test results, the expression of the remediation efficiency (RE) of Cr( ) contaminated specimen at different depths is as follows:

$$RE_X = \frac{m_{dx} - m_{fx}}{m_{dx}} \quad (2)$$

where x (cm) is specimen depth, $x = 0$ (the bottom of the specimen, in relation to the $FeSO_4$ inlet), 1.25, 2.5, 3.75, 5 cm in this study; RE_x is the remediation efficiency at depth x; m_{dx} (mg/kg) represents the Cr ( ) residual amount of the soil specimen at depth x cm in the control group (injection of distilled water); m_{fx} (mg/kg) represents the Cr( ) residual amount of the soil specimen at depth x cm under $FeSO_4$ injection.

2.5 Microstructure test

The surface morphology and elemental analysis of specimens after injected with $FeSO_4$ or distilled water under 100 kPa pressure were observed by Scanning electron microscopy with energy-dispersive X-ray spectroscopy (SEM-EDX, JSM-6700 F) at 15 KV operating voltage. The block specimens were polished to produce a smooth flat surface and were gold-coated for 30 s before SEM analysis.

3 Results And Discussion

3.1 Effects of $FeSO_4$ injection on hydraulic conductivity of Cr(□)-contaminated soil

When distilled water or $FeSO_4$ solution is injected into the specimen, the change of the hydraulic conductivity of silty clay contaminated with Cr( ) and the cumulative outflow volume for 24 hours under different pressures (30 kPa, 70 kPa, 100 kPa) are shown in Fig. 3.

As can be seen in Fig. 3, the hydraulic conductivities of the specimens injected with $FeSO_4$ solution were lower than that injected with distilled water. This was observed regardless of the injection pressure used. In particular, Fig. 3(a-c) indicates the hydraulic conductivity of the specimen with injection of distilled water initially increased and then gradually stabilized. However, the hydraulic conductivity of the

specimen with injection of $FeSO_4$ solution under 70 kPa and 100 kPa increased first and then decreased over time. These phenomena could be attributed to the following mechanisms. The initial increase in hydraulic conductivity might be due to the fact that the specimens are not fully saturated in a short time. With the continuous injection of $FeSO_4$ solution, Cr( ) was reduced by $FeSO_4$, forming a mixed iron( )/chromium( ) hydroxide [20]. Therefore, as time increased, the pores of the specimens were gradually blocked, and the hydraulic conductivity decreased with time until the chemical reaction reached an equilibrium.

The results present in Fig. 3d indicate that the saturated hydraulic conductivities of the specimens injected with distilled water under the pressure of 30 kPa, 70 kPa and 100 kPa were 3.475, 5.275, 5.235 $\times 10^{-7}$ cm/s, respectively and that injected with $FeSO_4$ solution were 2.205, 3.235, 3.55$\times 10^{-7}$ cm/s, respectively. In addition, for the injection pressure of 30 kPa, 70 kPa and 100 kPa, the hydraulic conductivity of the specimens injected with $FeSO_4$ decreased by 36.5%, 38.7% and 32.2%, respectively, compared with the specimens injected with distilled water. The lowest value was attained in 100 kPa, which could be attributed to difficult accumulation of precipitation in higher injection pressure. Moreover, the hydraulic conductivity of specimens injected with distilled water or $FeSO_4$ solution under the pressure of 30 kPa was lower than that under another two pressures (70 kPa, 100 kPa). By analyzing the relationship of the cumulative outflow volume with time under different injection pressures (Fig. 3(a-c)), it could be found that the cumulative outflow volume was not completely proportional to time. Thus, the lower hydraulic conductivity of the specimen at the injection pressure of 30 kPa might be due to the initial hydraulic gradient of the low permeability clayey soil. Only when the applied hydraulic gradient was greater than the initial hydraulic gradient, injection flow would be occurred. Another reason of that might be the short injection time and the hydraulic conductivity of the specimen at the lowest pressure (30 kPa) has not even reached stability.

3.2 Fe profiles in specimens after remediation by $FeSO_4$ under different injection pressures

Fe profiles in Cr ( )-contaminated specimens after remediation by $FeSO_4$ under different injection pressures are shown in Fig. 4.

The data from the post-remediation specimens over the 1.25-5.00 cm depth (from the bottom to the top of the specimen) indicated the increase in Fe concentration after $FeSO_4$ injection compared with the background value of Fe in the soil specimen (except for depth of 1.25 cm under 30 kPa). Moreover, the distribution of Fe concentration was dependent on the injection pressure of the $FeSO_4$ solution. Although the initial concentration distribution of Fe in different specimens was slightly different, in general, the higher the injection pressure, the higher the Fe concentration of the specimen at different depths.

It was found that the pH range of the outflow solution in this study was 3.44–5.65, which was much lower than the initial pH of precipitation of ferrous ion (Fe( )) in the solution. Therefore, the increase in Fe concentration should be attributed to the Fe( ) precipitation of formed by the redox reactions, not Fe( )

precipitation [20]. The higher iron increment indicated that there was enough Fe( ) to participate in the reduction reaction to form Fe( ), and the mobility capacity of Fe( ) was stronger. Based on the comparison of the Fe concentration in the specimen after remediation with $FeSO_4$ and that in the control specimen (injected with distilled water), the iron increment after remediation at different injection pressures was calculated. The results are presented in Table S2. It can be observed that the range of iron increment at 100 kPa was 3.2–11.9 (g/kg), while the maximum iron increment at 30 kPa was only 5 (g/kg), which means that the mobility capacity of Fe( ) was stronger under high pressure (100 kPa).

3.3 The remediation efficiency by injection of $FeSO_4$

The results of residual concentration of Cr in specimens after injected with $FeSO_4$ or distilled water for 24 h under different pressures (30 kPa, 70 kPa, 100 kPa) are shown in Fig. 5. Analyzing Fig. 5, it can be observed that the reduction of the Cr( ) was directly related to the injection pressure of $FeSO_4$ solution.

When the injection pressure of 30 kPa was adopted (Fig. 5a), the residual Cr( ) concentration of the specimen injected with $FeSO_4$ at the depths less than 2.5 cm was lower than that of the control specimen. While this was not the case when the depth was greater than 2.5 cm. It indicates that the migration of $FeSO_4$ was limited under the injection pressure of 30 kPa, which was less than 2.5 cm. Moreover, for the total chromium, the residual content increased with increasing depth when the specimen was injected with distilled water. This was due to the chromium migration with the injection flow from the bottom to the top of the specimen (5 cm depth) and accumulation occurred on the top surface. Meanwhile, this phenomenon was more obvious for the specimen after injected by $FeSO_4$. At the depths greater than 2.5 cm, the remediation might not occur and the leaching of the chromium was also limited owing to the lower permeability compared to the control specimen injected with distilled water. Therefore, at the depths greater than 2.5 cm, the residual chromium of the specimen injected with $FeSO_4$ was more than that of the control specimen.

When the $FeSO_4$ injection pressures of 70 kPa (Fig. 5b) and 100 kPa (Fig. 5c) were adopted, it was observed that the Cr( ) residual value was less than 20 mg/kg, which was below the risk intervention values for soil contamination of development land in China [27]. At a lower pressure (70 kPa), the residual value of Cr(VI) in the control specimen was more compared to that at the higher pressure of 100 kPa, which means that less Cr(VI) is leached in the specimen after injected by $FeSO_4$ under 70 kPa injection pressure. This is advantageous in actual remediation engineering because it will not cause the large expansion of the pollution plume during the injection process. Under 70 kPa and 100 kPa injection pressures, the residual concentration of total chromium in the specimen varied with depth in the same way. When injected with distilled water, the total chromium concentration gradually increased as the depth increased. However, when injected with ferrous sulfate, the total chromium concentration first decreased as the depth increased and then gradually stabilized. The concentration of total chromium in the specimen injected with ferrous sulfate was higher at the lower depth (in relation to the solution inlet) because a large amount of Cr( ) was reduced to Cr( ) and retarded at the bottom by the soil.

According to Eq. (2), the remediation efficiencies of Cr(VI) at different depths of the specimens under different injection pressures were calculated, and the results are shown in Fig. 6.

At the depths of 1.25 cm and 2.5 cm, the remediation efficiencies with injection pressure of 30 kPa were 22.76% and 97.03%, respectively. However, at the depths larger than 2.5 cm, the remediation efficiencies with the same pressure were negative. The lower hydraulic conductivity of the specimen injected with $FeSO_4$ resulted in low Cr( ) leaching ability. Meanwhile, the migration range of $FeSO_4$ under 30 kPa was less than 2.5 cm. Therefore, the residual Cr( ) concentration at the depth greater than 2.5 cm in the specimen after injected with $FeSO_4$ is higher than that of the control specimen. Moreover, the high remediation efficiency was achieved at the injection pressure of 70 kPa, which was 87.43%-95.12%. The remediation efficiency of 100 kPa injection pressure was lower than that of 70 kPa injection pressure, which could be attributed to the less amount of Cr( ) was reduced to Cr( ) by $FeSO_4$ due to the high Cr( ) leaching ability for the highest injection pressure. In summary, on the basis of setting the distilled water control test group, the remediation efficiency calculated by Eq. (2) can consider both Cr( ) reduction and Cr( ) leaching, and the actual remediation effect of the remediation agent can be evaluated. Thus, it could be concluded that the 70 kPa injection pressure was the most efficient under the experimental condition in this work. In addition, the remediation efficiency is not exactly proportional to the injection pressure because of the release of the contaminants under high injection pressure. The similar results were also obtained by Reginatto [28].

3.4 Microstructural investigations

Two representative soil specimens after injected with $FeSO_4$ or distilled water under 100 kPa pressure were used in the SEM-EDX analyses and the SEM images magnified by 200 times and 3000 times were obtained. The results are shown in Fig. 7.

As shown in Fig. 7a, a large number of pores of different lengths in specimen injected with distilled water were observed. Interestingly, denser surface could be observed in the specimen after injected with $FeSO_4$ solution (Fig. 7b). Figures 3 show that the hydraulic conductivity of the specimen injected with distilled water exhibited the higher value. Therefore, the surface morphology and microstructure of the specimens corresponded to the change of the hydraulic conductivity of the specimens when injected by $FeSO_4$ or distilled water. It also revealed that injection of $FeSO_4$ solution for remediation Cr( ) contaminated soil results in reducing the hydraulic conductivity of the soil.

SEM image of specimen injected with $FeSO_4$ at 3000 × magnification (Fig. 7b) indicated that the Fe( ) hydroxide might be formed and it filled the pores of the specimen. The identification was confirmed by elemental contents determined with EDX. The average iron weight percentage of the bright grey area as shown in Fig. 7b was 26.41%-30.46%, which was higher than that of the dark grey area, 12.63%.

4 Conclusions

Laboratory injection tests of $FeSO_4$ and distilled water were conducted to study the effect of injection pressure on remediation of clayey soil contaminated with Cr( ). The change of hydraulic conductivity of Cr( ) contaminated soil under the injection of the ferrous sulphate solution and distilled water were analyzed. The effects of different injection pressures on the migration and distribution of Fe at soils were discussed. In addition, SEM-EDX tests were also performed to reveal the mechanism of permeability variation of soil contaminated with Cr( ) during injection. The following conclusions can be drawn:

(1) Injection of $FeSO_4$ solution for remediation Cr( ) contaminated soil results in reducing the hydraulic conductivity of the soil. The hydraulic conductivity was decreased at the most by 38.7% at the 70 kPa injection pressure. During in situ application, field tests should be carried out to evaluate this impact and avoid clogging of the injection well.

(2) Fe profiles in specimens after remediation under different injection pressures were determined to analyze the migration depth of Fe( ). It indicated that the migration of Fe( ) was limited under the injection pressure of 30 kPa, which was less than 2.5 cm in this study. The mobility capacity of Fe( ) was stronger under higher pressure of 100 kPa.

(3) $FeSO_4$ is efficient for reducing Cr( ) in clayey soil. The high remediation efficiency (87.43%-95.12%) was achieved under 70 kPa injection pressure in this work. However, the remediation efficiency is not exactly proportional to the injection pressure. Excessive injection pressure will lead to the release of contaminants and spread the range of the pollution plume, while the distance for the remediation agent to migrate is limited.

(4) Cr( )-contaminated soil used in this study was prepared artificially and the relative content of exchangeable fraction chromium was high. The remediation effect of $FeSO_4$ on a real contaminated soil under higher injection pressure should be considered in the future. Moreover, the effect of concentration and pH of the solution should also be included at the same time.

Declarations

Data Availability

The data used to support the findings of this study are available from the corresponding author upon request.

Conflicts of Interest

The authors declare that they have no conflicts of interest.

Acknowledgments

The authors are grateful to the National Natural Science Foundation of China (Projects No. 42072318 & 41972282 & 41807253), the National Key Research and Development Program of China (Project No. 2019YFC1805905), Natural Science Foundation of Hunan Province, China (Project No. 2019JJ50763) for the financial support. And, also to grateful to the research fund program of the State Key Laboratory of Environmental Geochemistry (Project No. SKLEG2021208).

References

1. Y. He, B. B. Li, K. N. Zhang, Z. Li, Y. G. Chen, and W. M. Ye, “Experimental and numerical study on heavy metal contaminant migration and retention behavior of engineered barrier in tailings pond,” *Environmental Pollution*, vol. 252, pp. 1010-1018, 2019.
2. L. W. Liu, W. Li, W. P. Song, and M. X. Guo, “Remediation techniques for heavy metal-contaminated soils: Principles and applicability,” *Science of the Total Environment*, vol. 633, pp. 206-219, 2018.
3. D. O'Connor, X. D. Zheng, D. Y. Hou, Z. T. Shen, G. H. Li, G. F. Miao, S. O'Connell, and M. Guo, “Phytoremediation: Climate change resilience and sustainability assessment at a coastal brownfield redevelopment,” *Environment International*, vol. 130, pp. 104945, 2019.
4. L. Wang, L. B. Peng, L. L. Xie, P. Y. Deng, and D. Y. Deng, “Compatibility of Surfactants and Thermally Activated Persulfate for Enhanced Subsurface Remediation,” *Environmental Science & Technology*, vol. 51, pp. 7055-7064, 2017.
5. R. A. Wuana, F. E. Okieimen, B. Montuelle, and A. D. Steinman, “Heavy Metals in Contaminated Soils: A Review of Sources, Chemistry, Risks and Best Available Strategies for Remediation,” *ISRN Ecology*, pp. 402647, 2011.
6. L. Di Palma, D. Mancini, and E. Petrucci, “Experimental Assessment of Chromium Mobilization from Polluted Soil by Washing,” *Chemical Engineering Transactions*, vol. 28, pp. 145-150, 2012.
7. X. M. Zhao, P. A. Sobecky, L. P. Zhao, P. Crawford, M. T. Li, “Chromium (VI) transport and fate in unsaturated zone and aquifer: 3D Sandbox results,” *Journal of Hazardous Materials*, vol. 306, pp. 203-209, 2016.
8. L. Calder, “Chromium contamination of groundwater, in: J.O. Nrigagu, E.Nieboer (Eds.), Chromium in Natural and Human Environments,” *Advances in Environmental Sciences and Technology, Wiley, N.Y*, pp. 215–229, 1988.
9. K. GracePavithra, V. Jaikumar, P. S. Kumar, and P. SundarRajan, “A review on cleaner strategies for chromium industrial wastewater: Present research and future perspective,” *Journal of Cleaner Production*, vol. 228, pp. 580-593, 2019.
10. K. S. Padmavathy, G. Madhu, and P. V. Haseena, “A study on Effects of pH, Adsorbent Dosage, Time, Initial Concentration and Adsorption Isotherm Study for the Removal of Hexavalent Chromium (Cr (VI)) from Wastewater by Magnetite Nanoparticles,” *Procedia Technology*, vol. 24, pp. 585-594, 2016.
11. F. Kanwal, R. Rehman, T. Mahmud, J. Anwar, R. Ilyas, “Isothermal and Thermodynamical Modeling of Chromium (III) Adsorption by Composites of Polyaniline with Rice Husk and Saw Dust,” *Journal of*

the Chilean Chemical Society, vol. 57, no. 1, pp. 1058-1063, 2012.

12. L. Tofan, C. Paduraru, C. Teodosiu, O. Toma, "Fixed Bed Column Study on-the Removal of Chromium (III) Ions from Aqueous Solutions by Using Hemp Fibers with Improved Sorption Performance," *Cellulose Chemistry and Technology*, vol. 49, no. 2, pp. 219-229, 2015.
13. National RC, *Alternatives for Ground Water Cleanup*, The National Academies Press: Washington, DC, 1994.
14. Y. He, Y. G. Chen, and W. M. Ye, "Equilibrium, kinetic, and thermodynamic studies of adsorption of Sr(II) from aqueous solution onto GMZ bentonite," *Environmental Earth Sciences*, vol. 75, no. 9, pp. 807, 2016.
15. S. C. Ponce, C. Prado, E. Pagano, F. E. Prado, and M. Rosa, "Effect of solution pH on the dynamic of biosorption of Cr(VI) by living plants of Salvinia minima," *Ecological Engineering*, vol. 74, pp. 33-41, 2015.
16. H. Sharma, "Geoenvironmental Engineering: Site Remediation, Waste Containment and Emerging Waste Management Technologies," 2004.
17. I. Cecchin, C. Reginatto, W. Siveris, F. Schnaid, A. Thomé, and K. R. Reddy, "Remediation of Hexavalent Chromium Contaminated Clay Soil by Injection of Nanoscale Zero Valent Iron (nZVI)," *Water, Air, & Soil Pollution*, vol. 232, no. 7, pp. 286, 2021.
18. D. Dermatas and X. Meng, "Utilization of fly ash for stabilization/solidification (S/S) of heavy metal contaminated soils," *Engineering Geology*, vol. 70, no. 3, pp. 377-394, 2003.
19. C. Su and R. D. Ludwig, "Treatment of Hexavalent Chromium in Chromite Ore Processing Solid Waste Using a Mixed Reductant Solution of Ferrous Sulfate and Sodium Dithionite," *Environmental Science & Technology*, vol. 39, no. 16, pp. 6208-6216, 2005.
20. J. S. Geelhoed, J. C. L. Meeussen, M. J. Roe, S. Hillier, R. P. Thomas, J. G. Farmer, and E. Paterson, "Chromium Remediation or Release? Effect of Iron(II) Sulfate Addition on Chromium(VI) Leaching from Columns of Chromite Ore Processing Residue," *Environmental Science & Technology*, vol. 37, no. 14, pp. 3206-3213, 2003.
21. J. C. Seaman, P. M. Bertsch, and L. Schwallie, "In Situ Cr(VI) Reduction within Coarse-Textured, Oxide-Coated Soil and Aquifer Systems Using Fe(II) Solutions," *Environmental Science & Technology*, vol. 33, no. 6, pp. 938-944, 1999.
22. L. D. Palma, M. T. Gueye, and E. Petrucci, "Hexavalent chromium reduction in contaminated soil: A comparison between ferrous sulphate and nanoscale zero-valent iron," *Journal of Hazardous Materials*, vol. 281, pp. 70-76, 2015.
23. Y. He, W. M. Ye, Y. G. Chen, B. Chen, B. Ye, and Y. J. Cui, "Influence of pore fluid concentration on water retention properties of compacted GMZ01 bentonite", Applied Clay Science, vol. 129, pp. 131-141, 2016.
24. Y. He, W. M. Ye, Y. G. Chen, and Y. J. Cui, "Effects of K^+ solutions on swelling behavior of compacted GMZ bentonite," Engineering Geology, vol. 249, pp. 241-248, 2019.

25. US EPA, Method 3050 B: acid digestion of sediments, sludges and soils, 1996.
26. US EPA, Method 3060A: alkaline digestion for hexavalent chromium, 1996.
27. GB 36600-2018, Soil environmental quality Risk control standard for soil contamination of development land, 2018.
28. C. Reginatto, I. Cecchin, K. S. Heineck, A. Thomé, and K. R. Reddy, “Use of Nanoscale Zero-Valent Iron for Remediation of Clayey Soil Contaminated with Hexavalent Chromium: Batch and Column Tests”, INT J ENV RES PUB HE, 17(3):1-9, 2020.

Figures

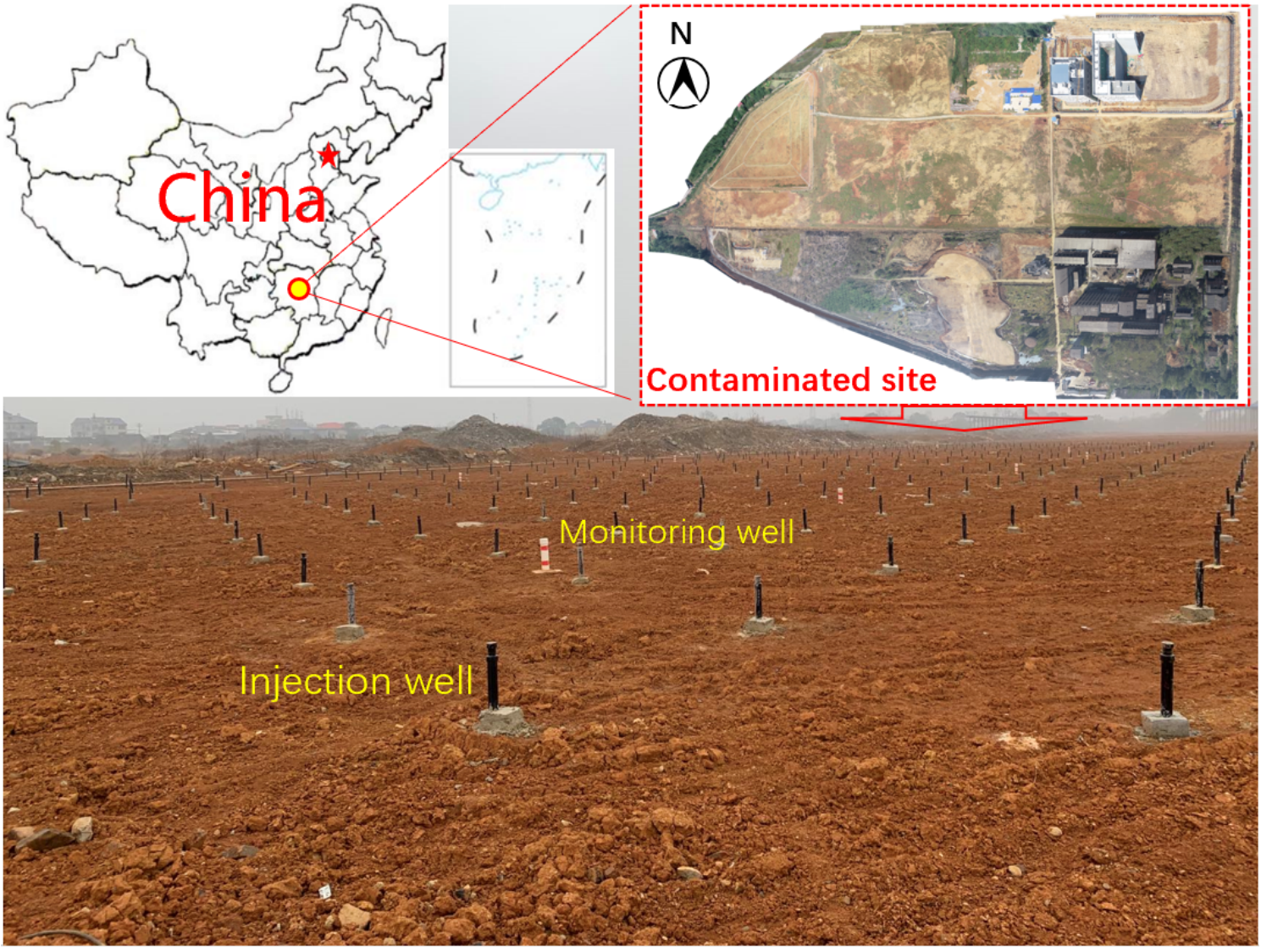

Figure 1

Specimen location

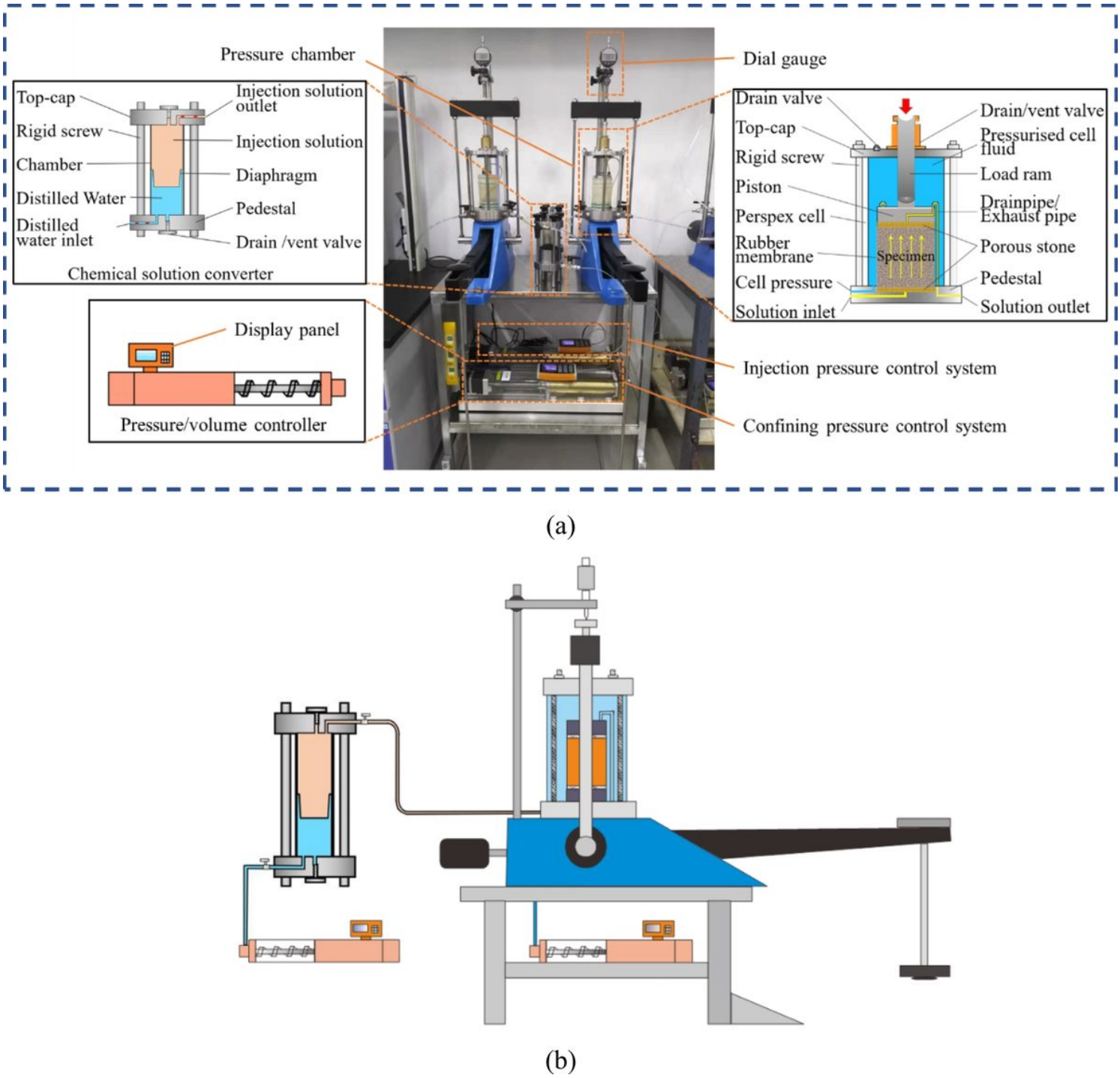

Figure 2

Design of injection system

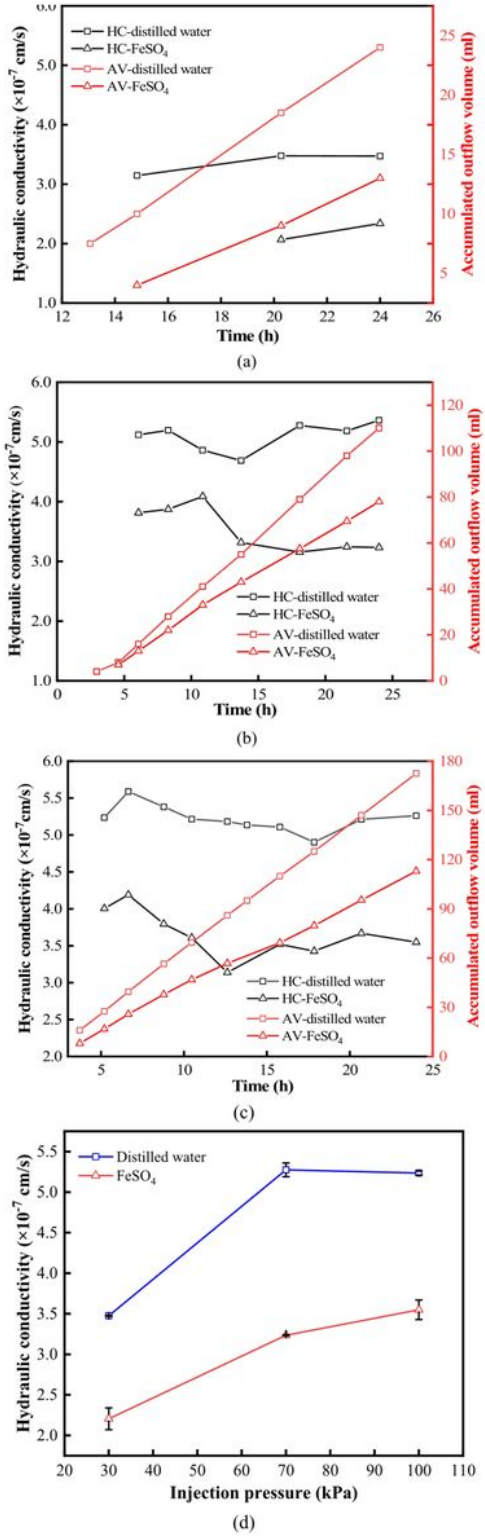

Figure 3

Hydraulic conductivity (HC) and accumulated outflow volume (AV) over time of the specimen injected with $FeSO_4$ or distilled water under different pressures (a) 30 kPa, (b) 70 kPa, (c) 100 kPa; (d) the effect of injection pressure on hydraulic conductivity under different pressures

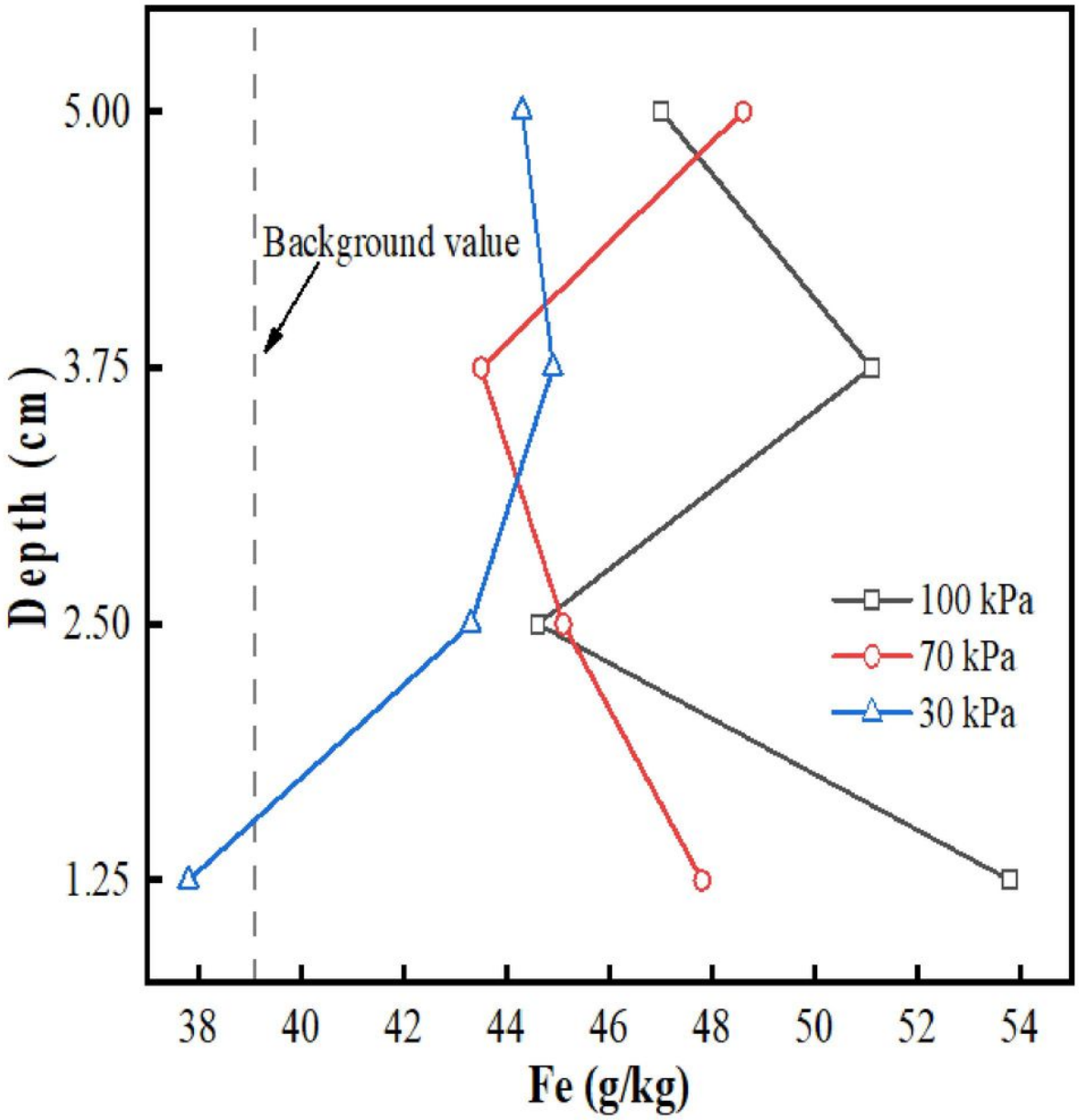

Figure 4

Fe concentration at different depths of the specimen under different $FeSO_4$-injection pressures

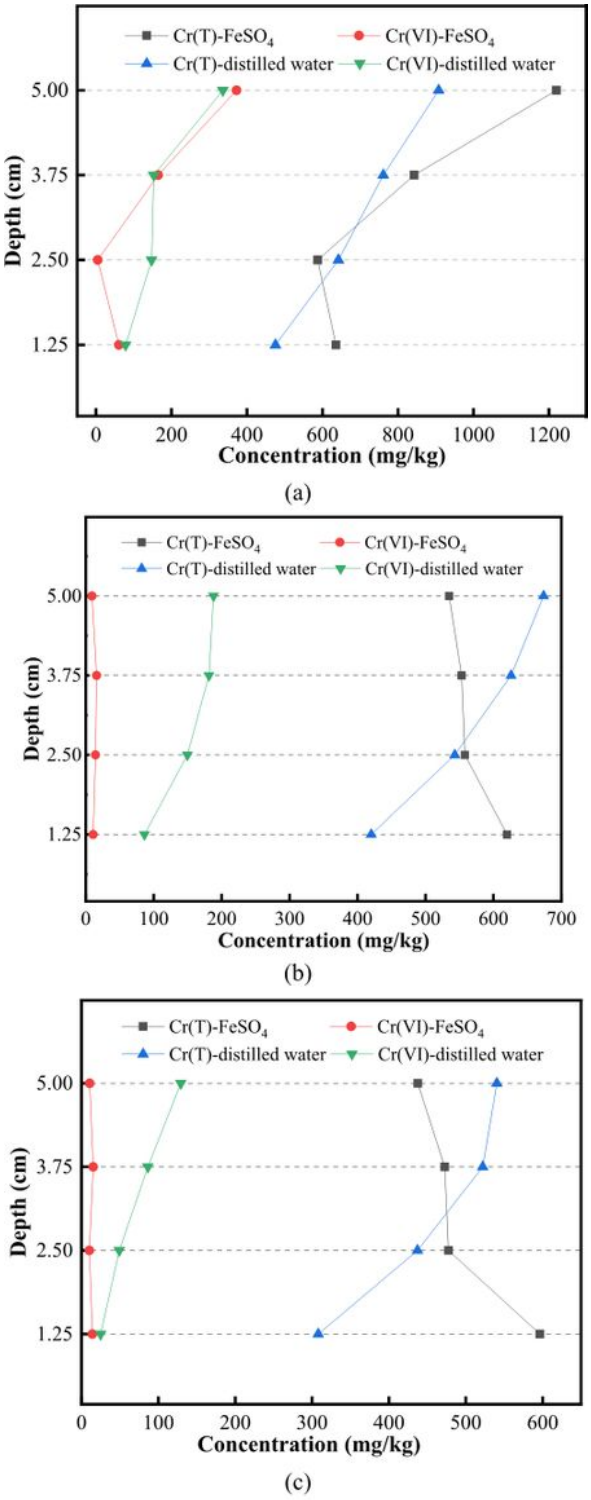

Figure 5

The residual concentration of Cr(Total) and Cr( ) at different depth of the specimens after injected with $FeSO_4$ or distilled water under pressures of: (a) 30 kPa; (b) 70 kPa; (c) 100 kPa.

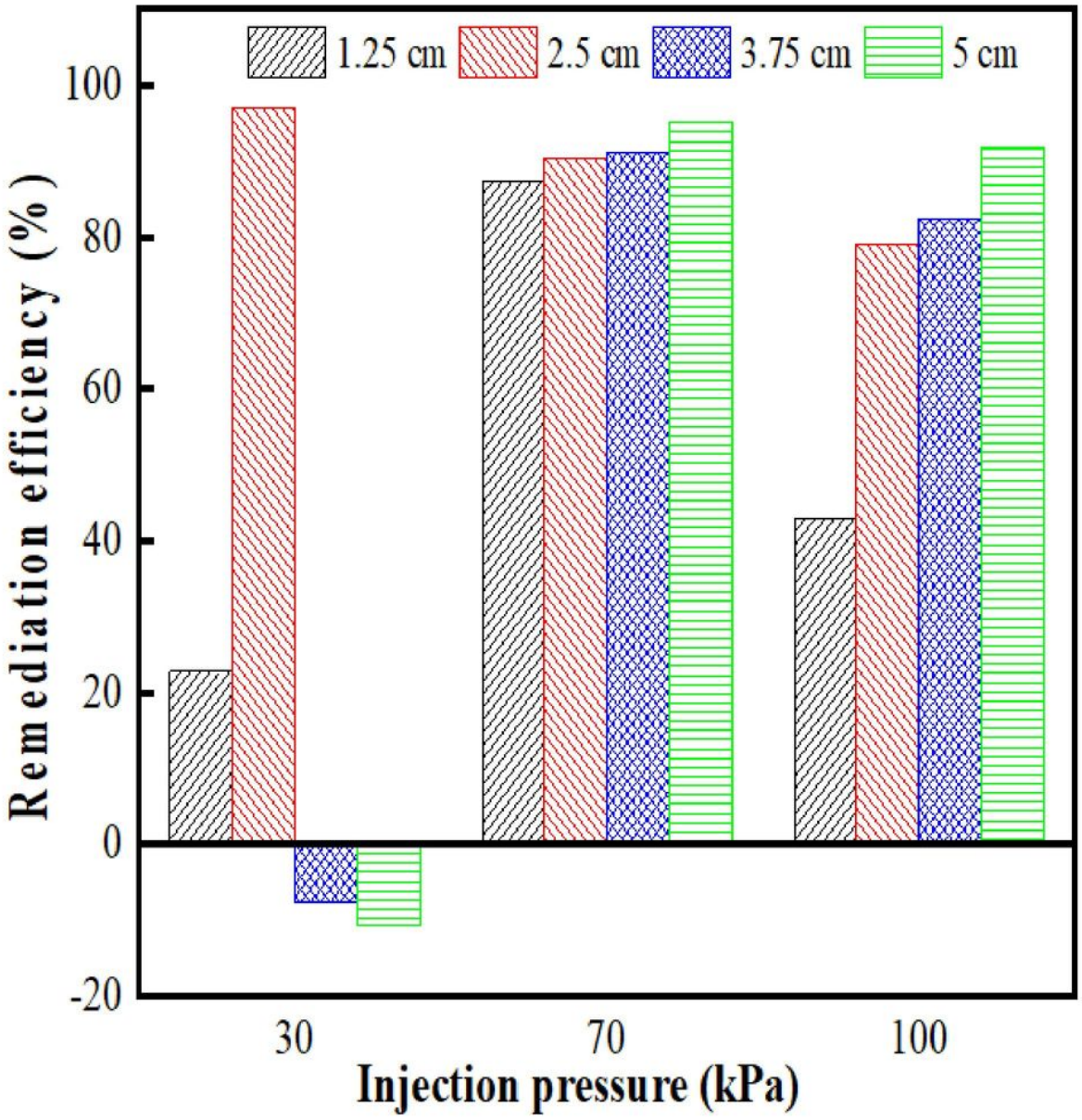

Figure 6

The remediation efficiencies of Cr(VI) at different depths of the specimens under different injection pressures

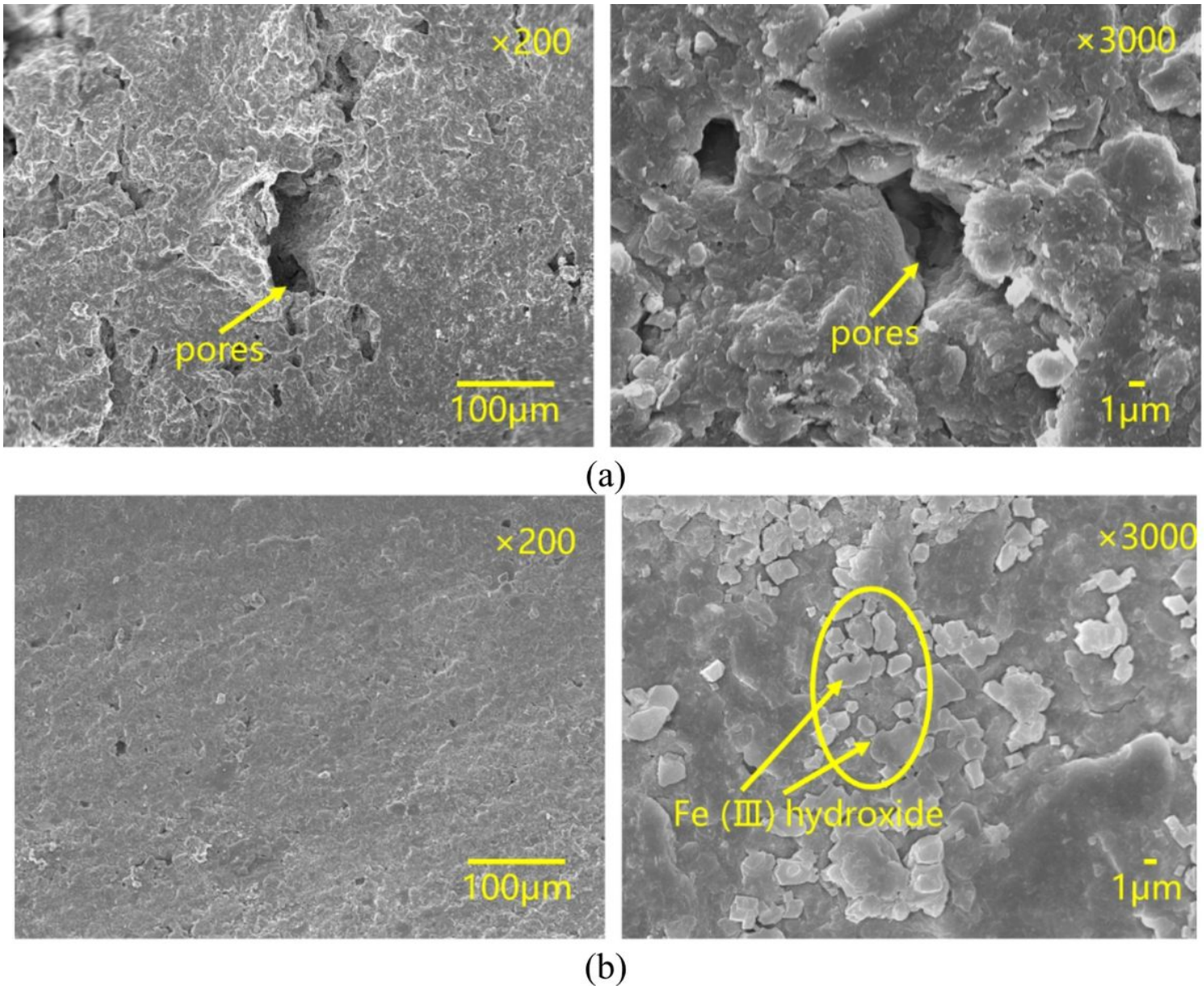

Figure 7

SEM results for the specimens: (a) SEM images of specimen after injected with distilled water; (b) specimen after injected with $FeSO_4$.

Supplementary Files

This is a list of supplementary files associated with this preprint. Click to download.

- Supplymentarymaterials.docx